The International Journal of Advanced Manufacturing Technology (2018) 97:3849–3857
https://doi.org/10.1007/s00170-018-2082-y

ORIGINAL ARTICLE

Fabrication of micro-textured surface using feed-direction ultrasonic vibration-assisted turning

Xianfu Liu[1,2] · Debao Wu[1,2] · Jianhua Zhang[1,2]

Received: 25 December 2017 / Accepted: 24 April 2018 / Published online: 2 June 2018

Abstract
Microstructures with proper patterns have an important influence on the functional surface performance of products, including changing surface wettability for different application environments. This paper proposed a method of feed-direction ultrasonic vibration-assisted turning (FUVAT) for fast generation of micro-textured surface. The generation mechanism of surface microstructures was presented by analyzing cutting trajectory and simulating surface topography. Surface texturing experiments were performed on copper 1100. The results show that micro-dimples with regular arrangement and different dimension were successfully obtained on cylindrical surface by controlling proper processing parameters. Several key parameters including amplitude, feed rate, and spindle speed play an important influence on the patterns and shapes of microstructures. The experimental textured surfaces show different wetting properties through wetting tests. It is verified that the FUVAT can be a feasible way to fabricate micro-textured surfaces.

Keywords Micro-textured surface · Feed-direction ultrasonic vibration-assisted turning · Surface generation mechanism · Wetting property

1 Introduction

Micro-textured surfaces with proper patterns and shapes of microstructures are widely used to improve the functional performance of parts [1]. In many biomedical and industrial applications, the method of modifying the surface microstructures to change the wetting property has become an important way to fabricate superhydrophobic or hydrophilic surfaces [2, 3]. For examples, windshields with the superhydrophobic textured surfaces possess self-cleaning function in an automobile [4] and titanium alloys with hydrophilic textured surfaces can enhance the adhesive bonding [5]. With the increasing application of textured surfaces, it is necessary to develop a cost-effective and efficient method to generate microstructures on surfaces [6].

Vibration-assisted cutting (VAC) technique is a combined machining method, which changes the material removal mechanism from continuous cutting to intermittent cutting by applying ultrasonic vibration to one or more directions of the tool or workpiece [7]. Compared with conventional cutting, VAC has obvious advantage in machining difficult-to-machine material [8–10], reducing cutting force [11], improving tool life [12], and achieving better surface finishing [13]. Recent years, with ever-growing demand for micro-textured surface processing technology, the VAC technique has been used to fabricate microstructures on surfaces, especially for elliptical vibration cutting [14]. Among which, Guo [15, 16] proposed a method of elliptical vibration texturing to generate microstructures on cylindrical surfaces and systematically studied the influence of different microstructures on the wettability of textured surfaces; Xu [6, 17, 18] successfully applied a novel rotary ultrasonic texturing method to fabricate different tailored microstructures on flat and inner cylindrical surfaces with one-point diamond tool recently.

Nevertheless, there are few researches on the generation of textured surface using one-dimensional vibration-assisted

✉ Jianhua Zhang
jhzhang@sdu.edu.cn

[1] Key Laboratory of High Efficiency and Clean Mechanical Manufacture, Ministry of Education of China, School of Mechanical Engineering, Shandong University, Jinan 250061, China

[2] National Demonstration Center for Experimental Mechanical Engineering Education, School of Mechanical Engineering, Shandong University, Jinan 250061, China

cutting so far, although Schubert et al. [19–21] studied the micro-structured surfaces generated by ultrasonic vibration cutting in cutting direction, radial direction, and feed direction, respectively. However, the feed rate was much larger than the vibration amplitude in the feed-direction vibration-assisted cutting. As a result, the wide and deep grooves on surfaces were not removed because of the little influence of vibration amplitude. Considering the ultrasonic vibration in feed direction can change the feed rate and cutting trajectory, which can result in the change of surface topography, the paper proposed the method of feed-direction ultrasonic vibration-assisted turning (FUVAT) to fabricate micro-textured surfaces. This method includes only one-dimensional ultrasonic vibration, whose advantages are fast generation and simple processing. Unlike previous studies, the feed rate and vibration amplitude of FUVAT have the same order of magnitude, which can fabricate different patterns and shapes of microstructures and generate more regular micro-textured surfaces. The texturing generation mechanism was analyzed and textured surfaces were fabricated successfully in experimental tests. The wetting properties of micro-textured surfaces were also measured and analyzed to provide a foundation for further application of the FUVAT technique.

2 Generation mechanism of micro-textured surface

2.1 Textured generation procedure

Figure 1 shows the process of FUVAT. Workpiece rotates at a speed of n around Z-axis. The ultrasonic vibration is added to make the cutting tool vibrate in feed direction. The ultrasonic vibration in the feed direction periodically changes the feed rate and the resulting feed rate can be calculated according to the following formula [19]:

$$S_v = S + A\sin(2\pi ft) \tag{1}$$

where S_v is the resulting feed rate, S is the initial feed rate, A is the vibration amplitude, and f is the frequency of ultrasonic vibration. The maximum fluctuation range of feed rate is 2A. The cutting tool can make a sinusoidal movement along the cutting direction.

Figure 2 shows the cutting motion trajectory of FUVAT on the Y-Z plane. There are four parameters influencing the motion trajectory of cutting edge, including A, S, φ, and d_c. φ is the phase difference between two adjacent cutting trajectories, which can be expressed as follows:

$$\varphi = \left\{ \frac{60 \times f}{n} - \left[\frac{60 \times f}{n} \right] \right\} \times 2\pi \tag{2}$$

where f is the ultrasonic frequency and n is the spindle speed. d_c is the dimension of one vibration cycle in cutting direction, which can be calculated by the following:

$$d_c = V_c / f \tag{3}$$

where V_c is the cutting speed.

The cutting motion trajectory can be controlled by choosing proper processing parameters, which results in the fabrication possibility of micro-textures on cylindrical surface. Figure 3 shows the motion trajectory of the cutting tool controlled by adjusting ultrasonic amplitude under given ultrasonic frequency, feed rate, and phase difference. When 2A = S and $\varphi = \pi$, the adjacent cutting trajectories are in critical crossing state; when 2A < S and $\varphi = \pi$, the adjacent cutting

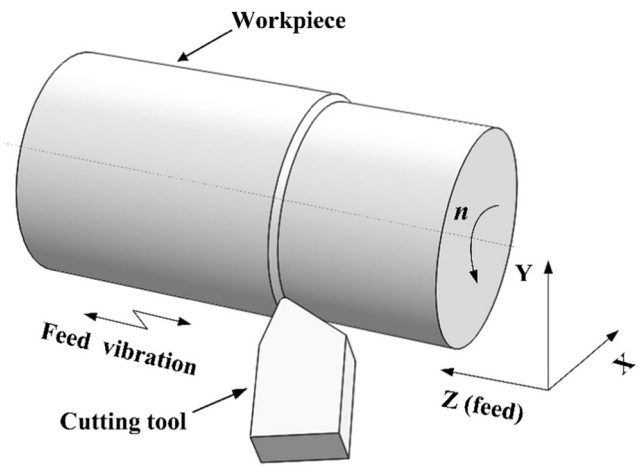

Fig. 1 Schematics of the FUVAT process

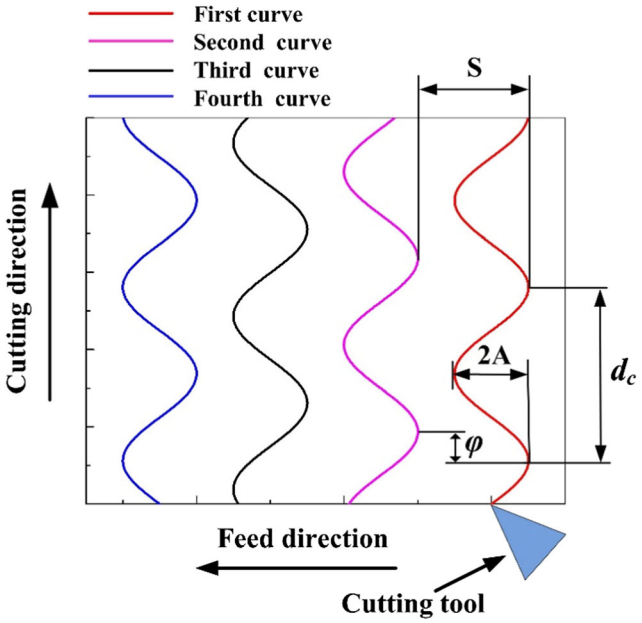

Fig. 2 Motion trajectory of the cutting tool

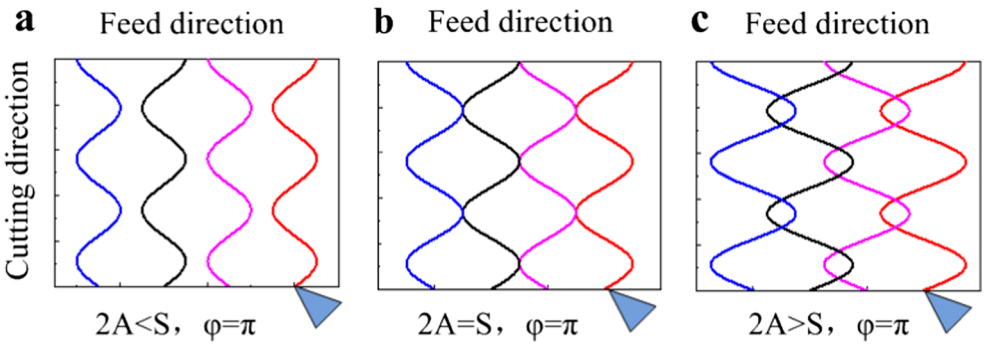

Fig. 3 Cutting trajectory under different ultrasonic amplitudes

trajectories do not present crossing state; and when $2A > S$ and $\varphi = \pi$, the adjacent cutting trajectories are in obvious crossing state. The workpiece can obtain various surface topographies by changing the cutting trajectory in FUVAT.

2.2 Simulation analysis of surface topography generation

For better understanding and prediction of micro-textured surface generation in FUVAT, a surface topography generation model is used to simulate the FUVAT progress and the 3D surface topography. The model was obtained by revised Guo' and Sajjady' models [15, 22] which were not used to simulate textured surfaces in the process of ultrasonic vibration-assisted cutting in feed direction. To simplify the algorithm program of the surface topography generation model, the minimum chip thickness and elastic recovery are not considered in the current simulation algorithm. In the simulation model, the tool geometry parameters, including the rake angle, nose radius, and clearance angle, are determined according to the actual tool used in experimental tests. The rake angle, clearance angle, and nose radius are 0°, 7°, and 100 μm, respectively. Besides, in the simulation process of FUVAT, the dimeter of workpiece is 22 mm, the ultrasonic vibration frequency is 20 kHz, the depth of cut (DOC) is 0.2 mm, and the amplitude is kept at 10 μm.

The surface topography generation model is realized by the Matlab program. Figure 4 shows the 3D surface topography of FUVAT under different parameters. Figure 4(a–c) shows the surface topography influenced by different feed rates under

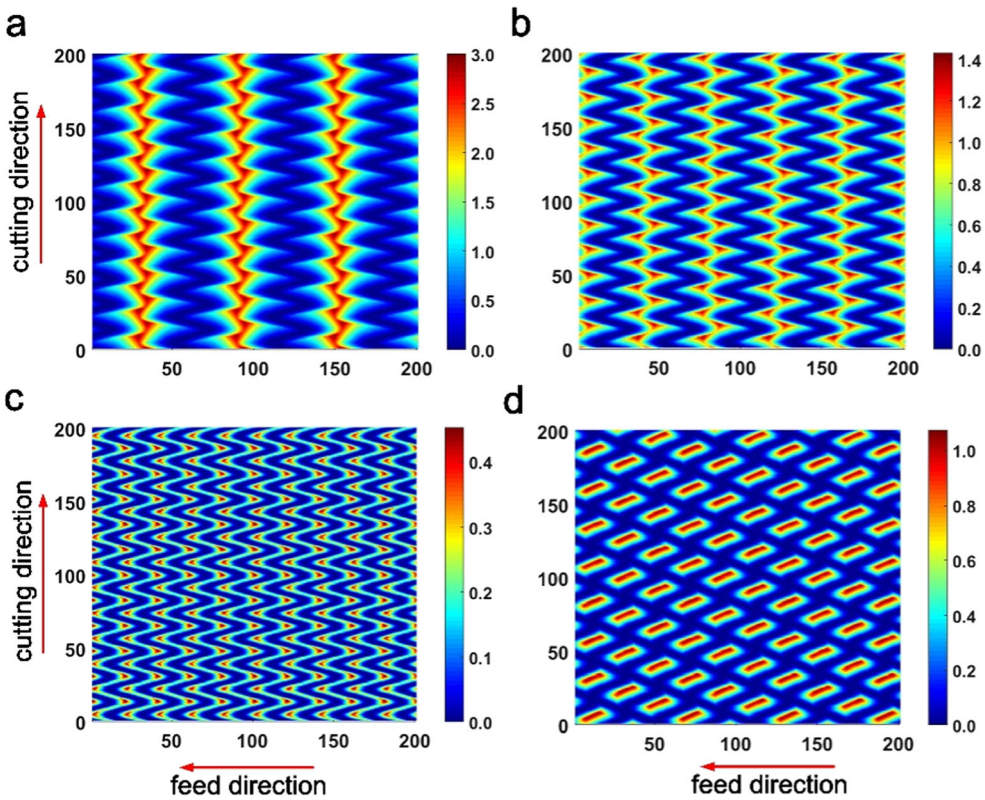

Fig. 4 3D simulation surfaces of FUVAT under different parameters. (**a**) $n = 300$ r/min, $\varphi = 0$, $S = 60$ μm/rev. (**b**) $n = 300$ r/min, $\varphi = 0$, $S = 40$ μm/rev. (**c**) $n = 300$ r/min, $\varphi = 0$, $S = 20$ μm/rev. (**d**) $n = 450$ r/min, $\varphi = 1.3\pi$, $S = 20$ μm/rev

DOC of 0.2 mm, amplitude of 10 μm, and spindle speed of 300 r/min. It can be seen that a sinusoidal ridge is generated between grooves. The width of the formed sinusoidal ridge is determined by the feed rate mainly. With decreasing in the feed rate, the influence of amplitude on the sinusoidal ridge becomes more and more obvious. As shown in Fig. 4(c, d), with spindle speed increasing from 300 to 450 r/min, the distribution of textured surfaces changes from a sinusoidal pattern to a protruding pattern because of the changing of φ increasing from 0 to 1.3π. The distance between the adjacent protruding ridge along the cutting direction is equal to d_c, and therefore the patterns become sparse because of the increasing of spindle speed.

The textured surfaces can be theoretically obtained by simulation results of the surface topography. It provides a basis for further experimental study on the micro-textured surface generated by FUVAT. In the following, experimental tests were carried out to fabricate microstructures on cylindrical surface.

3 Experimental details

The experimental setup for the FUVAT process is shown in Fig. 5. The experimental tests were carried out on a CNC lathe (PRECION, CKD6150H). The ultrasonic transducer with vibration frequency of 20 kHz was mounted on platform of the CNC lathe through a base. An intelligent ultrasonic generator is used to provide the power to the ultrasonic transducer. The range of ultrasonic amplitude is from 0 to 10 μm. The spindle speeds were set around 300, 450, and 600 r/min. The depth of cut was set at 0.2 mm. The feed rates were set at 20, 40, and 60 μm/rev.

The investigations of micro-textured surfaces generated by FUVAT were carried out on the copper 1100 because of its good ductility. To eliminate the eccentricity as far as possible, the cylindrical copper workpiece was firstly pre-turned to reach the external diameter of 22 mm without ultrasonic vibrations. The cutting insert (Sandvik Coromant, DCGT11T301) was a cemented carbide tool with a nose radius of 100 μm. The rake and clearance angle of the cutting tool were 0° and 7°, respectively. All the experimental conditions of FUVAT were summarized in Table 1.

4 Results and discussions

4.1 Experimental micro-textured surface

4.1.1 Effect of amplitude

A laser microscope (KEYENCE, VK-9700) was used to observe and analyze the surfaces fabricated by FUVAT. Figures 6(a, b) and 7 show the surfaces generated by FUVAT under ultrasonic amplitudes of 0, 5, and 10 μm, respectively. Figure 6(a) shows the surface topography when amplitude is 0 μm, which is equivalent to the conventional turning process. Because that wear and peeling factors exist in the cutting process of copper 1100, the surface shows a row of irregular grooves. On the contrary, when the amplitudes are 5 and 10 μm, cylindrical surfaces with different regular microstructures were successfully fabricated, which were shown in Figs. 6(b) and 7, respectively. From Fig. 6(b), it can be observed that the textured surface with sinusoidal ridges was fabricated. With the amplitude increasing to 10 μm, the microstructures of textured surface become compactly arranged dimples because of the change of cutting trajectory, as shown in Fig. 7(a). The distance between the arranged dimples along the feed

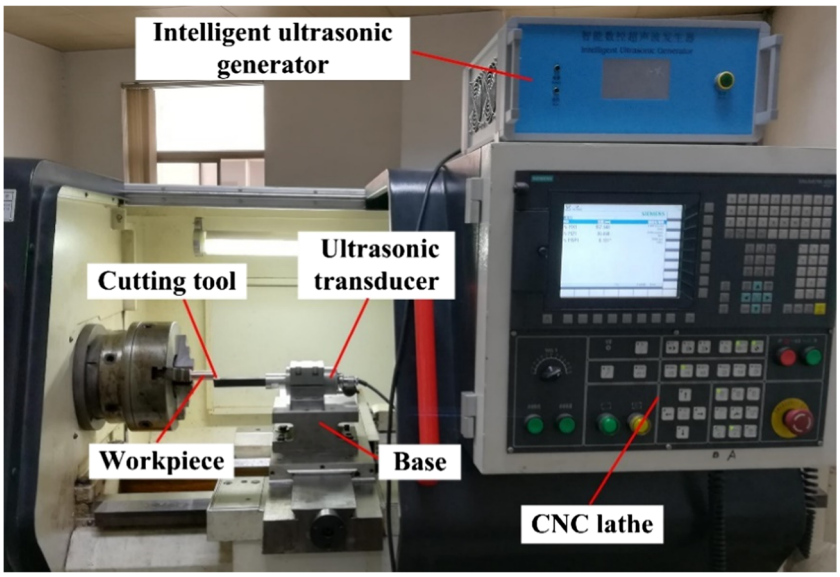

Fig. 5 Experimental setup for the FUVAT process

Table 1 Experimental conditions

Tool geometry	Material	Cemented carbide
	Rake angle (°)	0
	Clearance angle (°)	7
	Nose radius (μm)	100
Workpiece	Material	Copper 1100
	Diameter (mm)	22
Machining conditions	Vibration frequency (kHz)	20
	Vibration amplitude (μm)	0, 5, 10
	Spindle speed (r/min)	300, 450, 600
	Feed rate (μm/rev)	20, 40, 60
	DOC (depth of cut) (mm)	0.2

direction is 20 μm, which is determined by the feed rate. Figure 7(b) shows the cross-sectional profile of arranged dimples along the cutting direction. Through measurement, the average values of d_1 (dimension between adjacent dimples) and d_{p1} (depth of dimple) are 17.2 and 0.6 μm, respectively. Under the same processing parameters, d_c is calculated to be 17.3 μm through Eq. (3), which is approximately equal to d_1. Therefore, the dimension between adjacent dimples along the cutting direction is determined by the cutting speed and ultrasonic frequency. The cross-sectional profile exists some small fluctuation, as shown in the red circle area in Fig. 7(b). This is due to the cutting scratches caused by friction during the process of the material removal, which is shown in the yellow circle area. It can be found from Figs. 6 to 7 that regular textured surfaces can be fabricated by changing the ultrasonic amplitude.

4.1.2 Effect of spindle speed

When DOC is 0.2 mm, the feed rate is 20 μm/rev, and amplitude is 10 μm, micro-textured surfaces fabricated under the spindle speeds of 450 and 600 r/min were shown in Figs. 8 and 9, respectively. Compared with Fig. 7, the patterns of microstructures become sparser in the cutting direction and regular elliptical dimples cover the cylindrical surface. The average values of d_2, d_{p2}, d_3, and d_{p3} were measured to be 24.6, 1.1, 32.5, and 1.0 μm, respectively. The depths of dimples generated under 450 and 600 r/min are approximately the same, but they are greater than those of dimples generated under 300 r/min. This is because that the edge of dimples generated under 300 r/min has more cutting scratches compared with others, which results in the smaller depth. The values of d_c under 450 and 600 r/min are calculated to be 25.9 and 34.5 μm, which are basically consistent with d_2 and d_3, respectively. With the

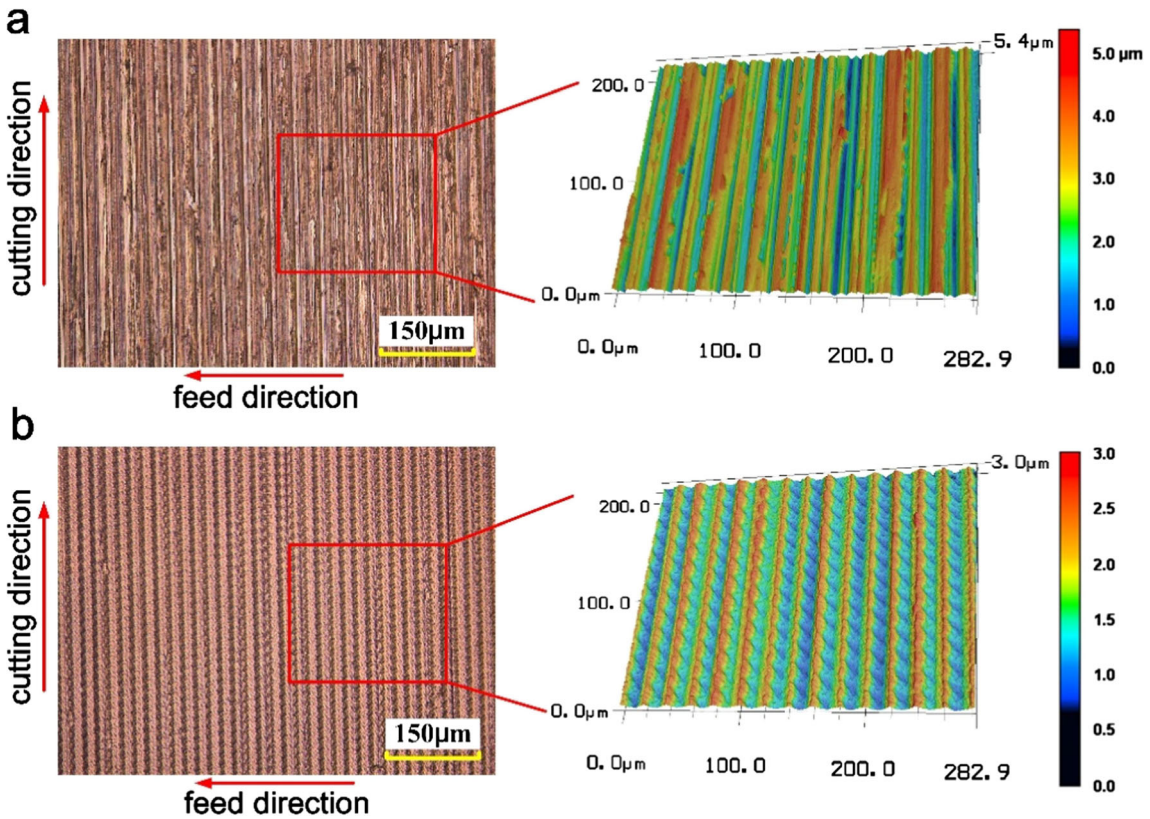

Fig. 6 Surfaces fabricated by FUVAT under processing parameters of $n = 300$ r/min, DOC = 0.2 mm, and $S = 20$ μm/rev. (**a**) $A = 0$ μm. (**b**) $A = 5$ μm

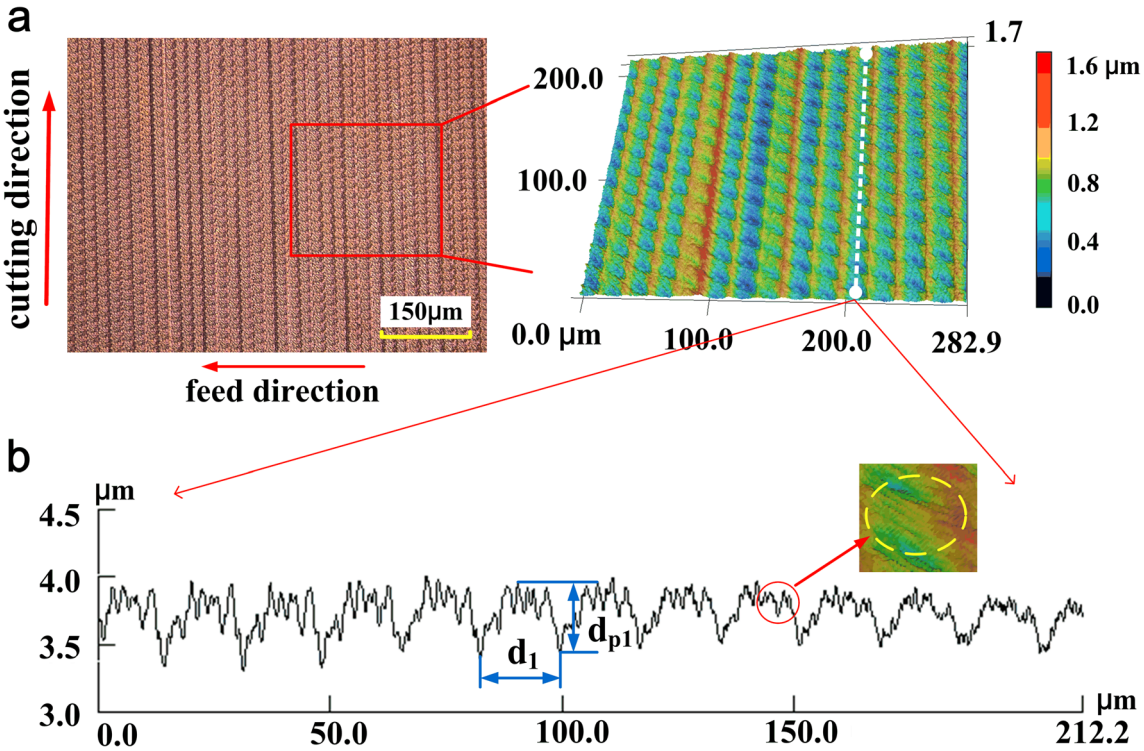

Fig. 7 Micro-textured surface fabricated by FUVAT ($n = 300$ r/min, DOC = 0.2 mm, $S = 20$ μm/rev, $A = 10$ μm): (**a**) surface topography and (**b**) the cross-sectional profile along the cutting direction

spindle speed increasing from 300 and 450 to 600 r/min, the dimension between adjacent dimples correspondingly becomes from 17.2 and 24.6 to 32.5 μm owing to the increasing of d_c. Therefore, the spindle speed has an important influence on the arrangement of microstructures along cutting direction.

4.1.3 Effect of feed rate

When DOC is 0.2 mm, spindle speed is 300 r/min, and amplitude is 10 μm, surfaces fabricated under feed rate of 40 and 60 μm/rev were shown in Fig. 10(a, b), respectively. Different from the micro-textured surface generated under the feed rate

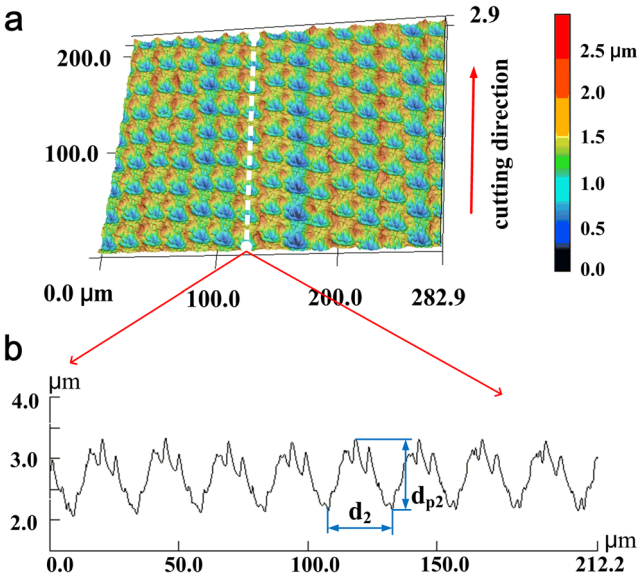

Fig. 8 Micro-textured surface fabricated by FUVAT ($n = 450$ r/min, DOC = 0.2 mm, $S = 20$ μm/rev, $A = 10$ μm): (**a**) surface topography and (**b**) the cross-sectional profile along the cutting direction

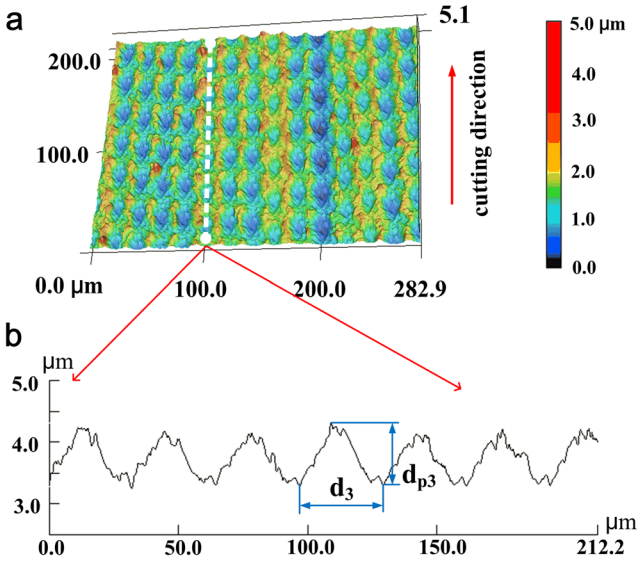

Fig. 9 Micro-textured surface fabricated by FUVAT ($n = 600$ r/min, DOC = 0.2 mm, $S = 20$ μm/rev, $A = 10$ μm): (**a**) surface topography and (**b**) the cross-sectional profile along the cutting direction

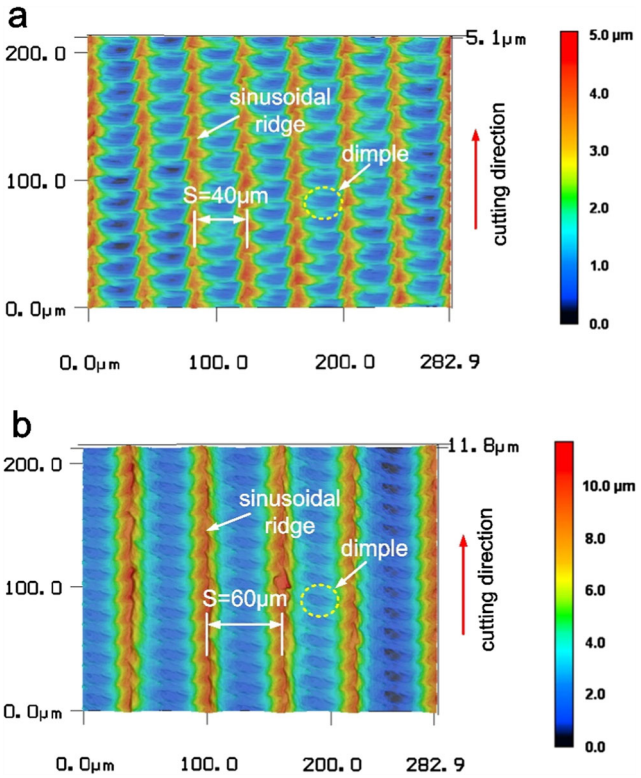

Fig. 10 Surfaces fabricated by FUVAT under processing parameters of $n = 300$ r/min, DOC = 0.2 mm, and $A = 10$ μm. (**a**) $S = 40$ μm/rev. (**b**) $S = 60$ μm/rev

of 20 μm/rev, the dimples became less highlighted and were replaced by obvious grooves gradually with the increasing of feed rate. An apparent sinusoidal ridge was also generated between grooves because of the sinusoidal cutting path. When amplitude remains unchanged and feed rate increases, the influence of amplitude on generating microstructures becomes more and more small. Therefore, only when feed rate and amplitude have the approximately same order of magnitude, micro-dimples with regular patterns and shapes can be fabricated by FUVAT.

4.2 Comparison of experimental and simulation results

By comparing the surface topographies in Fig. 4(a, b) with those in Fig. 10(a, b), simulation topography is similar to experimental topography when feed rates are 40 and 60 μm/rev, respectively. A small difference is that the widths of the experimental sinusoidal ridge were measured to be 22.3 and 26.5 μm respectively, which are less than those of simulation. This is caused by the possible reducing of amplitude under loading and extruding peeling of material. However, when feed rate is 20 μm/rev, experimental topography shows big difference with simulation topography apparently, by comparing Fig. 4(c, d) with Figs. 7 and 8, respectively. One difference is that cutting scratches were

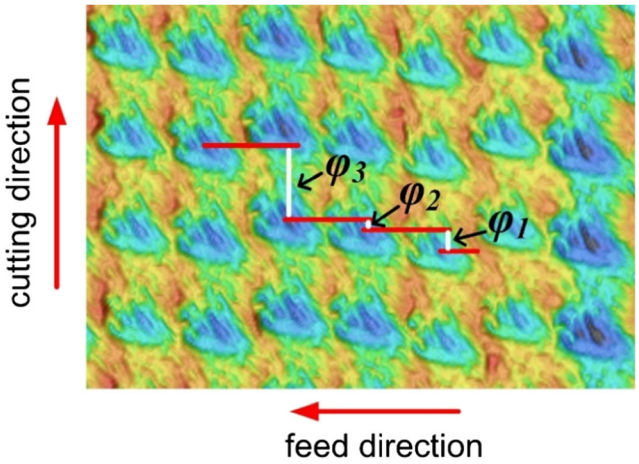

Fig. 11 The adjusting φ in experimental textured surface ($n = 450$ r/min, DOC = 0.2 mm, $S = 20$ μm/rev, $A = 10$ μm)

created at the surface of microstructures of experimental tests, which can be the result of cutting friction during material removal. Another difference is that experimental textured surfaces were covered with regular dimples; on the contrary, the simulation surfaces in Fig. 4(c, d) were covered with sinusoidal grooves and protruding patterns, respectively. This is because of the following reasons: The simulation is based on a simplified model without considering minimum chip thickness, elastoplastic deformation, and adhesion of tool which exist in the real process of FUVAT; the variance of spindle speed is about ±2% in the CNC lathe, resulting in the actual bias of φ, which can be verified by adjusting φ ($\varphi_1 \neq \varphi_2 \neq \varphi_3$) in the experimental textured surface, as shown in Fig. 11. Because of the large plastic deformation of copper 1100 and the impactive shear extrusion process of the cutting tool, the protruding ridges may be connected together to form dimples. Furthermore, for predicting the surface topography of FUVAT accurately, a more optimized model needs to be established in the future research work.

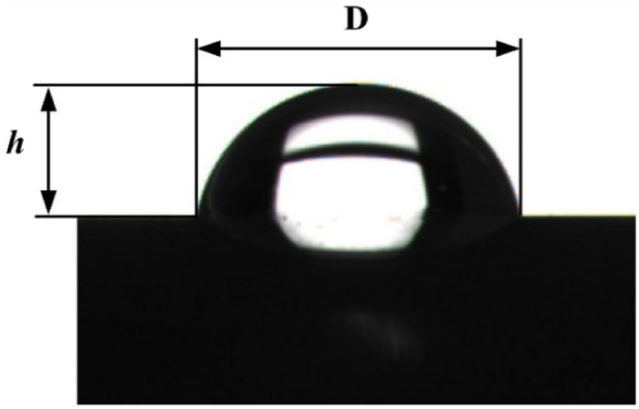

Fig. 12 Schematic of water contact angle measurement on cylindrical surface

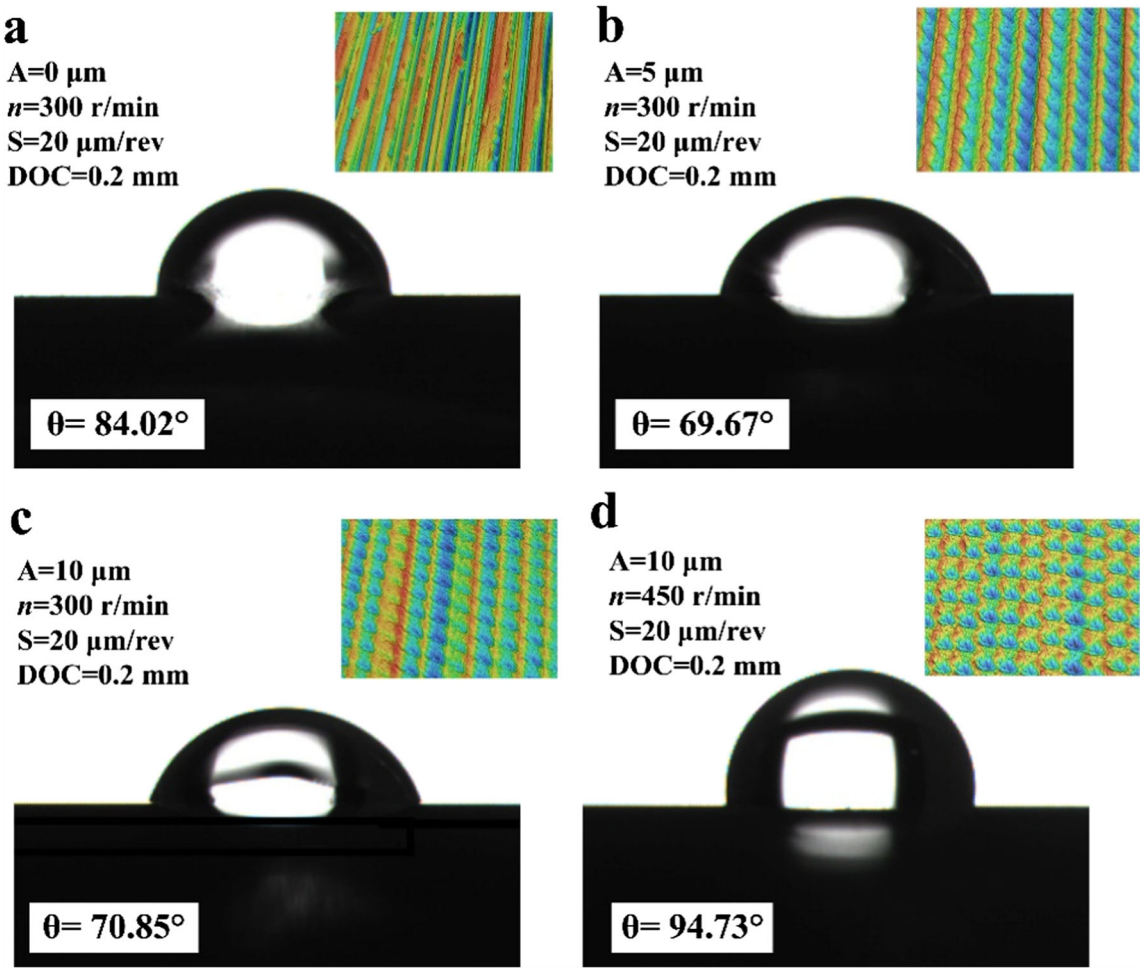

Fig. 13 Water contact angles of four surfaces fabricated by FUVAT

4.3 Wetting properties

To study the wetting properties of textured surfaces generated by FUVAT, a professional water contact angle measurement device (POWEREACH, JC2000D1) was used to carry out the wettability tests. Before the tests, the samples were cleaned in an ultrasonic clean machine with alcohol for 30 min to wash off any residual chips and dried in air environment for 60 min. The water used in the wettability tests was deionized water and the volume of water droplets was all kept at 2 μL. To reduce the random errors, each surface was measured four times and the mean value was taken as the final experimental result. The sessile drop method was used to calculate the water contact angle in feed direction to evaluate the wetting properties of cylindrical surfaces, which is shown in Fig. 12. The water contact angle can be calculated according to the following formula [23]:

$$\theta = 2\arctan\left(\frac{2h}{D}\right) \tag{4}$$

where h and D are the height and width of the water droplet, respectively.

The measured water droplet angles of four surfaces fabricated by FUVAT are shown in Fig. 13. Compared with the surface fabricated by the turning without ultrasonic vibration, it can be found that the hydrophilicities of two textured surfaces are enhanced because of the water contact angles decreasing from 84.02° to 69.67° and 70.85° respectively, as shown in Fig. 13(a, c). On the contrary, another textured surface with the water contact angle of 94.73° shows stronger hydrophobicity than others owing to the sparse patterns and regular elliptical dimples, as shown in Fig. 13(d). From the analysis of measurement results, the microstructures on cylindrical surfaces fabricated by the FUVAT have an important influence on the wettability.

5 Conclusions

Based on the results and analysis in the present paper, the following conclusions can be drawn.

1. Simulation results preliminarily proved the theoretical feasibility of the FUVAT in generating micro-textured surfaces on the whole.

2. Micro-textured surfaces were fabricated successfully through experimental tests of the FUVAT. The ultrasonic amplitude, feed rate, and spindle speed play an important influence on the patterns and shapes of microstructures. Regular arrangement of micro-dimples can be generated, when feed rate is 20 μm/rev and amplitude is 10 μm (peak-to-peak is 20 μm), which have the approximately same order of magnitude. With the increasing of spindle speed, the dimension between adjacent dimples along cutting direction increases.
3. According to wetting tests, the experimental textured surfaces present different wetting properties, which provides a foundation for further application. Different hydrophilic or hydrophobic surfaces can be obtained through changing processing parameters of the FUVAT.
4. The FUVAT is proved to be a relatively simple and effective way to fabricate micro-textured surfaces. The advantage of this method is that the process only needs one step—that is, adding ultrasonic vibration to feed direction of the conventional turning.

Funding information This work was supported by the National Science Fund of China (NSFC), No. 51475275.

References

1. Bruzzone AAG, Costa HL, Lonardo PM, Lucca DA (2008) Advances in engineered surfaces for functional performance. CIRP Ann Manuf Technol 57(2):750–769
2. Li XM, Reinhoudt D, Crego-Calama M (2007) What do we need for a superhydrophobic surface? A review on the recent progress in the preparation of superhydrophobic surfaces. Chem Soc Rev 36: 1350–1368
3. Baburaja EG, Starikov D, Evans J, Shafeev GA, Bensaoula A (2007) Enhancement of adhesive joint strength by laser surface modification. Int J Adhes Adhes 27(4):268–276
4. Quere D (2005) Non-sticking drops. Rep Prog Phys 68(11):2495–2532
5. Rotella G, Alfano M, Candamano S (2015) Surface modification of Ti6Al4V alloy by pulsed Yb-laser irradiation for enhanced adhesive bonding. CIRP Ann Manuf Technol 64(1):527–530
6. Xu SL, Shimada K, Mizutani M, Kuriyagawa T (2017) Development of a novel 2D rotary ultrasonic texturing technique for fabricating tailored structures. Int J Adv Manuf Technol 89: 1161–1172
7. Brehl DE, Dow TA (2008) Review of vibration-assisted machining. Precis Eng 32(3):153–172
8. Kumabe J, Fuchizawa K, Soutome T, Nishimoto Y (1989) Ultrasonic superposition vibration cutting of ceramics. Precis Eng 11(2):71–77
9. Zhou M, Wang XJ, Ngoi BKA, Gan JGK (2002) Brittle-ductile transition in the diamond cutting of glasses with the aid of ultrasonic vibration. J Mater Process Technol 121:243–251
10. Liu K, Li XP, Rahman M (2008) Characteristics of ultrasonic vibration-assisted ductile mode cutting of tungsten carbide. Int J Adv Manuf Technol 35(7):833–841
11. Zhou M, Eow YT, Ngoi BK, Lim EN (2003) Vibration-assisted precision machining of steel with PCD tools. Mater Manuf Process 18(5):825–834
12. Zhou M, Ngoi BKA, Yusoff MN, Wang XJ (2006) Tool wear and surface finish in diamond cutting of optical glass. J Mater Process Technol 17:29–33
13. Moriwaki T, Shamoto E (1991) Ultraprecision diamond turning of stainless steel by applying ultrasonic vibration. CIRP Ann Manuf Technol 40(1):559–562
14. Zhang JG, Cui T, Ge C, Sui YX, Yang HJ (2016) Review of micro/nano machining by utilizing elliptical vibration cutting. Int J Mach Tools Manuf 106:109–126
15. Guo P, Ehmann KF (2013) An analysis of the surface generation mechanics of the elliptical vibration texturing process. Int J Mach Tools Manuf 64:85–95
16. Guo P, Lu Y, Ehmann KF, Cao J (2014) Generation of hierarchical micro structures for anisotropic wetting by elliptical vibration cutting. CIRP Ann Manuf Technol 63:553–556
17. Xu SL, Shimada K, Mizutani M, Kuriyagawa T (2014) Fabrication of hybrid micro/nano-textured surfaces using rotary ultrasonic machining with one-point diamond tool. Int J Mach Tools Manuf 86: 12–17
18. Xu SL, Shimada K, Mizutani M, Kuriyagawa T (2016) Analysis of machinable structures and their wettability of rotary ultrasonic texturing method. Chin J Mach Eng 29(6):1187–1192
19. Schubert A, Nestler A, Pinternagel S, Zeidler H (2011) Influence of ultrasonic vibration assistance on the surface integrity in turning of the aluminium alloy AA2017. Mater Werkst 42(7):658–665
20. Nestler A, Schubert A (2014) Surface properties in ultrasonic vibration assisted turning of particle reinforced aluminium matrix composites. Procedia CIRP 13:125–130
21. Zhang R, Steinert P, Schubert A (2014) Microstructuring of surfaces by two-stage vibration assisted turning. Procedia CIRP 14: 136–141
22. Sallady SA, Nouri Hossein Abadi H, Amini S, Nosouhi R (2016) Analytical and experimental study of topography of surface texture in ultrasonic vibration assisted turning. Mater Design 93:311–323
23. Qin LG, Lin P, Zhang YL, Dong GN, Zeng QF (2013) Influence of surface wettability on the tribological properties of laser textured Co–Cr–Mo alloy in aqueous bovine serum albumin solution. Appl Surf Sci 268:79–86